Current Drug Discovery Technologies, 2022, *19*, e231221199369

RESEARCH ARTICLE

Extracting Atomic Contributions to Binding Free Energy Using Molecular Dynamics Simulations with Mixed Solvents (MDmix)

Daniel Alvarez-Garcia[1], Peter Schmidtke[2,†], Elena Cubero[1] and Xavier Barril[1,2,3,*]

[1]*Gain Therapeutics, Parc Cientific de Barcelona, Baldiri Reixac 10, 08029 Barcelona, Spain;* [2]*Facultat de Farmacia, Universitat de Barcelona, Av. Joan XXIII 27-31, 08028 Barcelona, Spain;* [3]*Catalan Institution for Research and Advanced Studies (ICREA), Passeig Lluis Companys 23, 08010 Barcelona, Spain*

ARTICLE HISTORY

Received: August 06, 2021
Revised: September 02, 2021
Accepted: October 05, 2021

DOI:
10.2174/1570163819666211223162829

Abstract: ***Background*:** Mixed solvents MD (MDmix) simulations have proved to be a useful and increasingly accepted technique with several applications in structure-based drug discovery. One of the assumptions behind the methodology is the transferability of free energy values from the simulated cosolvent molecules to larger drug-like molecules. However, the binding free energy maps (ΔG_{bind}) calculated for the different moieties of the cosolvent molecules (*e.g.* a hydroxyl map for the ethanol) are largely influenced by the rest of the solvent molecule and do not reflect the intrinsic affinity of the moiety in question. As such, they are hardly transferable to different molecules.

***Method*:** To achieve transferable energies, we present here a method for decomposing the molecular binding free energy into accurate atomic contributions.

***Result*:** We demonstrate with two qualitative visual examples how the corrected energy maps better match known binding hotspots and how they can reveal hidden hotspots with actual drug design potential.

***Conclusion*:** Atomic decomposition of binding free energies derived from MDmix simulations provides transferable and quantitative binding free energy maps.

Keywords: Mixed solvents, MD simulations, structure-based drug discovery, binding free energy, atomic contribution, MDmix.

1. INTRODUCTION

Predicting the binding free energy (ΔG_{bind}) of a drug candidate (ligand) to its pharmacological target (receptor) is the holy grail of structure-based drug design. The ΔG_{bind} of two molecules engaged in a non-covalent complex has a univocal relationship with the equilibrium constant ($K_A = 1/K_D = \exp(-\Delta G_{bind}/RT)$), which is the experimental observable. Thus, computational chemistry methods strive to predict ΔG_{bind} in the hope that one day it will be possible to design drugs on the computer. Traditional methods, such as MM-PBSA [1] or the scoring functions implemented in docking software [2], aim to predict ΔG_{bind} from the protein-ligand interactions. However, such methods cannot properly take into account the effect of the solvent and the configurational diversity of the bound and unbound states (ensembles). As a result, they often deliver mediocre results. Molecular dynamics (MD) simulations, combined with the impressive software and hardware developments of the last decades, have opened the possibility of observing binding and unbinding events of a protein-ligand system and, thus, a direct route to the calculation of the binding constant [3]. When executed properly, this offers the most accurate results, well within the experimental error [4]. However, this is impractical for drug-like ligands because: i) many binding and unbinding events must be observed in order to attain statistically meaningful binding constants, and ii) potent ligands exhibit slow (dissociation) kinetics, resulting in binding half-lives longer than the simulation times currently amenable [5]. Solutions to this limitation have been proposed [6-8], but calculating ΔGbind for a single molecule of interest is a major effort even in the best case. In order to exploit this powerful approximation in a practical way, we and others proposed the use of MD simulations with mixed aqueous/organic solvents (MDmix) [9, 10] due to their small size, organic solvents display, fast diffusion, and binding rates. Furthermore, they can be simulated at relatively high concentrations (1 % to 20 %), which facilitates rapid convergence of the simulations. While the organic solvents *per se* are of no interest, the information they provide can be very useful. Indeed, experimentally it has been observed that organic solvents can be used to detect binding hotspots, thus pinpointing the functional sites of proteins [11, 12]. MDmix-type methods have become very popular, with an expanding number of applications that range from the original use in druggability prediction to receptor-based pharmacophore discovery, identification of displaceable water molecules, elucidation of cryptic pockets, or as a scoring func-

*Address correspondence to this author at the Gain Therapeutics, Parc Cientific de Barcelona, Baldiri Reixac 10, 08029 Barcelona, Spain; E-mail: xbarril@gaintherapeutics.com

† *Current address: Discngine, 79 Avenue Ledru Rollin, 75012 Paris, France*

tion for docking (for an extensive review, see reference [13]). However, all these applications rely on a crucial assumption: the transferability of the ΔG_{bind} obtained for the organic solvents to larger ligands. Group transferability has a long tradition in drug design. As a notable example, the Free-Wilson analysis relies on this particular assumption to derive quantitative structure-activity relationships (QSAR) [14]. But the ΔG_{bind} values derived from MDmix simulations reflect the contribution of the entire solvent molecule. In order to obtain quantitative values, it is necessary to partition this magnitude into group contributions that are more accurate and transferable. In this article, we outline a rigorous partitioning method of our device [15], which we have been using very successfully for the discovery of allosteric pharmacological chaperones. First, we will outline the method. Then we will provide examples to illustrate its utility.

2. METHODS

The first step in MDmix is to prepare a system of interest (usually a biological macromolecule) for MD simulation in the usual way. Then the system is solvated using a pre-equilibrated solvent box containing a mixture of water and the organic solvent that will be used as a probe (*e.g.*, ethanol). Next, a sufficiently long MD trajectory is produced. This generally involves multiple independent replicas that will be analysed together. In the final step, the space around the system is partitioned into volume elements (voxels), and the ΔG_{bind} of the solvent at each voxel is calculated from its observed density [16]. At the first order, the atomic contribution to ΔG_{bind} of atom *i* (ΔG^{i}_{bind}) is calculated using the expression:

$$\Delta G^{i}_{bind} = -k_B T \ln(N_i/N_o) \quad (1)$$

where k_B is the Boltzmann constant, T is the temperature at which the simulation was run, N_i is the number of times that a particular group has fallen in a volume element, and N_o is the expected value if there were no contribution from the macromolecule. However, this assumes that each atom moves freely, which is clearly not the case for polyatomic molecules.

The MDmix method uses amphiphilic organic molecules to probe the interaction preferences of the biological macromolecule of interest. The use of amphiphilic molecules (*i.e.*, those containing a polar head combined with a hydrophobic tail) provides two important advantages. On the one hand, due to their polar head, they are more soluble than purely hydrophobic solvents and can be simulated at higher concentrations (thus ensuring faster convergence) without the need for artificial potentials that prevent phase separation [10]. More importantly, the polar groups of organic molecules (*e.g.*, a hydroxyl) behave quite differently than a purely polar solvent (*e.g.*, water). Thus, the use of amphiphilic organic molecules is necessary to reliably identify and quantify polar interactions [17]. The downside to this choice is that binding to the surface of the macromolecule is the result of the interactions formed by each of the groups (hydrophobic and hydrophilic), which can be quite distinct. Fig. (**1**) (top) illustrates three ideal cases with the same total (molecule-based) ΔG_{bind}, but disparate group contributions. In the first case (Fig. **1A**), both probe atoms make equally favourable contacts with the protein, and ΔG_{bind} is evenly distributed amongst them. In the second case (Fig. **1B**), only one group is making favourable contacts, while the other prefers to remain solvated, making no effective contribution to the total ΔG_{bind}. The third case (Fig. **1C**) represents an intermediate situation, where one group makes the most important interaction, while the second group explores several energetically favourable positions. As shown, the group contributions (ΔG^{i}_{bind}) calculated using Equation 1 contain significant errors, because the observed densities for one atom are largely influenced by the interaction preferences of the other one (*i.e.*, the assumption that the atoms move independently is not true). In order to obtain accurate and transferable group contributions, it becomes necessary to decouple the binding of the polar head from the binding of the hydrophobic tail. This can be done based on the relative densities of each group: those establishing stronger interactions will exhibit larger densities compared to the others. Fig. (**1**) (bottom) shows that atomic contributions (ΔG^{i}_{bind}) calculated in this way also have an artefactual dependency on the size of the molecule: irrespective of the chemical character of the atoms, bigger molecules can attain larger total ΔG_{bind} (absolute) values. This translates into larger observed densities of individual atoms, even if the atomic contributions (*i.e.*, ligand efficiencies) are not better. The repartitioning scheme must be able to correct both of these situations, providing truly atom-specific contributions. As such, they should not surpass the experimentally-observed maximal atomic contributions, which rarely reach -1.0 kcal/mol and have a physical limit at -1.5 kcal/mol [18].

The decoupling procedure devised here is based on a comparison of the uncorrected atomic ΔG^{i}_{bind} values with the expected value considering the ΔG_{bind} of the entire molecule (ΔG^{M}_{bind}). Firstly, we must calculate ΔG^{i}_{bind} and ΔG^{M}_{bind} using Equation 1. In the former case, we use the coordinates of the atomic nuclei to calculate densities and in the latter, the coordinates of the centre of mass (CoM) of the entire molecule. From ΔG^{M}_{bind}, we obtain the expected atomic contribution:

$$\Delta G^{i}_{0} = \Delta G^{M}_{bind} * \alpha^{i} \quad (2)$$

Where α^{i} is the fraction of ΔG^{M}_{bind} contributed by atom *i* in the ideal situation where all atoms of the molecule contribute equally to the binding. For instance, in a molecule formed by N identical atoms (*e.g.*, benzene, N=6), each atom would have an α value of 1/N. For molecules with non-identical atoms, several partitioning schemes are possible. For simplicity, let us assume that ΔG_{bind} is proportional to the solvent accessible surface area (SASA). Then, we can define α^{i} as the SASA fraction of atom *i* in molecule *M*:

$$\alpha^{i} = SASA^{i} / SASA^{M} \quad (3)$$

Note that, for flexible molecules, the SASA values should be averaged over all three-dimensional conformations (weighted by population). The corrected contribution of a particular atom can then be calculated as the uncorrected value minus the expected contribution of the rest of the molecule:

$$\Delta G^{i}_{corr} = \Delta G^{i}_{bind} - (\Delta G^{M}_{bind} - \Delta G^{i}_{0}) \quad (4)$$

Fig. (**1**) illustrates the impact of this correction in idealised systems. Since the CoM of the molecule can explore a

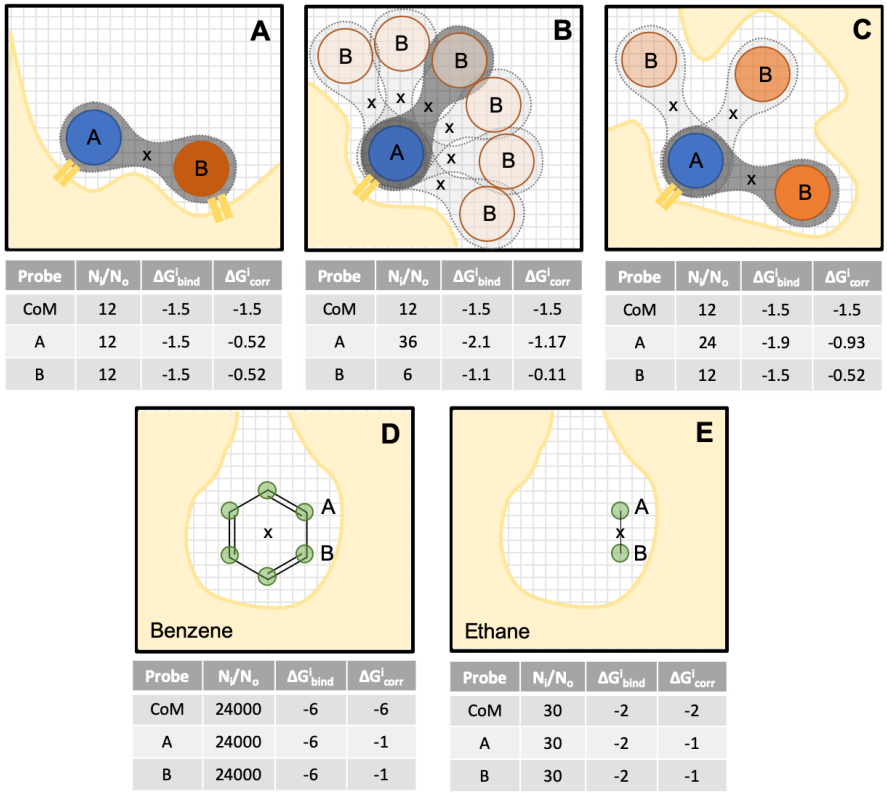

Probe	N_i/N_o	ΔG^i_{bind}	ΔG^i_{corr}
CoM	12	-1.5	-1.5
A	12	-1.5	-0.52
B	12	-1.5	-0.52

Probe	N_i/N_o	ΔG^i_{bind}	ΔG^i_{corr}
CoM	12	-1.5	-1.5
A	36	-2.1	-1.17
B	6	-1.1	-0.11

Probe	N_i/N_o	ΔG^i_{bind}	ΔG^i_{corr}
CoM	12	-1.5	-1.5
A	24	-1.9	-0.93
B	12	-1.5	-0.52

Probe	N_i/N_o	ΔG^i_{bind}	ΔG^i_{corr}
CoM	24000	-6	-6
A	24000	-6	-1
B	24000	-6	-1

Probe	N_i/N_o	ΔG^i_{bind}	ΔG^i_{corr}
CoM	30	-2	-2
A	30	-2	-1
B	30	-2	-1

Fig. (1). Calculation of atomic contributions to ΔG_{bind} on idealised systems. **Top:** Idealised 3-atom molecule bearing a hydrophobic head (atom A; blue; $\alpha^A = 0.35$) and a polar tail (atom B; orange; $\alpha^B = 0.35$). Total ΔG^M_{bind} (as calculated from the density of the CoM (marked as **x**)) is the same in all cases, but they differ on the relative atomic densities. The tables show the raw (ΔG^i_{bind}) and corrected (ΔG^i_{corr}) atomic contributions for a particular binding mode of the molecule (dark-shaded background). **Bottom:** Size dependency of ΔG^i_{bind} illustrated on an idealised site where benzene attains a total $\Delta G^M_{bind} = 6$ kcal/mol, and all atoms contribute equally. Two molecular probes of the same character but different sizes (benzene and ethane) afford very different ΔG^i_{bind} but identical ΔG^i_{corr} values. Protein surface is shown in ochre. The grid represents space discretization into volume elements (*A higher resolution / colour version of this figure is available in the electronic copy of the article*).

range of positions when atom *i* localizes in a particular voxel, it is necessary to re-analyse the simulation, identifying the location of the CoM at each snapshot during the trajectory. The reported ΔG^i_{corr} for a particular voxel is the average value across all snapshots in the simulation:

$$\langle \Delta G^i_{corr} \rangle = \sum \Delta G^i_{corr} / N_i \quad (5)$$

Where the summation runs from 1 to N_i (*i.e.*, the number of times that atom *i* has fallen into that voxel). In the next section, we showcase two real case examples to demonstrate the power of the correction.

3. RESULTS

3.1. Example 1: Hsp90

Hsp90 is an oncology target that has become a testbed for structure-based drug design [19]. The primary interaction point in the active site of Hsp90, used by almost all known ligands, is the side-chain of Asp93, which acts as a powerful hydrogen bond acceptor [20]. We ran an MD simulation of the N-terminal domain of Hsp90 in apo form (initial structure 2XDK) [21] in a mixture of 20 % v/v isopropanol/water mixture (equilibrated solvent box available for download at: http://mdmix.sourceforge.net). Then, the contributions to binding free energy were calculated using Eq. 1 on a cubic grid spanning the entire protein surface (grid spacing = 0.5Å in each dimension) for the methyl atoms (hydrophobic probe), the hydroxyl atom (polar probe), and the central atom (used as a proxy of the CoM). Fig. (**2**) shows the isocontour (surface encompassing voxels with equal values) of the hydrophobic probe at ΔG_{bind} = -1.5 kcal/mol (blue mesh). Note that this value is at the physical limit identified by Kuntz and Kollman [18], revealing that it is an overestimate caused by the use of a 4-atom molecule, as explained above. This visualization technique reveals five preferred binding sites (hot spots) for the hydrophobic probe. Four of them are in good agreement with the placement of hydrophobic moieties by known ligands. But the one closer to Asp93 overlaps with the preferred positions of polar atoms and can be attributed to the tight binding between the polar probe and Asp93 (similar to the situation described in Fig. **1B**). After correction (red surface isocontour), this presumed binding hot spot disappears, confirming that it was largely caused by the interaction preferences of the polar head rather than intrinsic interaction preferences of the hydrophobic tails. Interestingly, the same correction expands the hydrophobic hot spot at the bottom of the image, while the other three sites are not significantly affected by the correction. Note that the values depicted in this case (ΔG_{corr} = -0.7 kcal/mol) are in much better agreement with

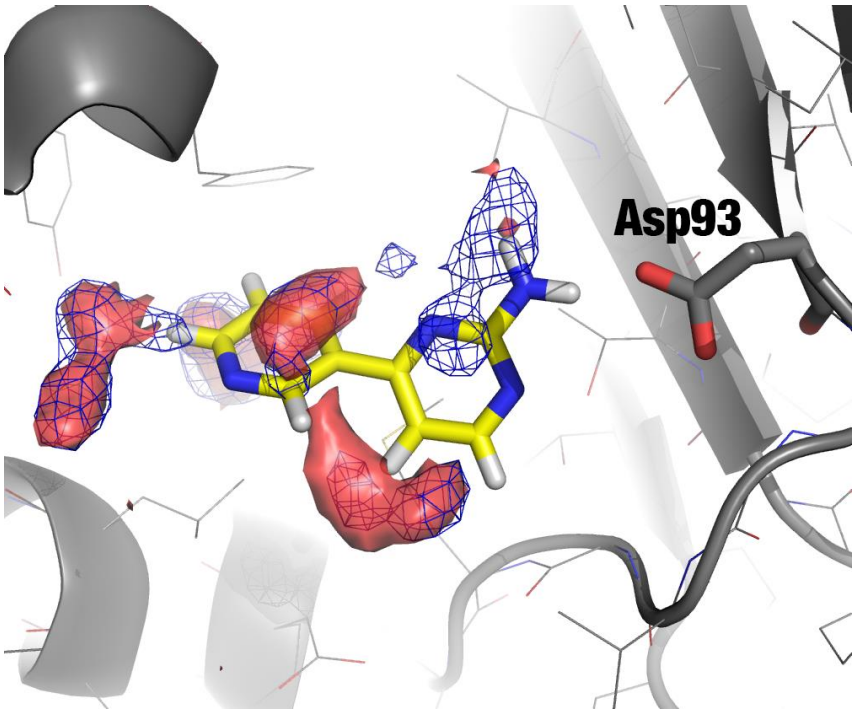

Fig. (2). Contour plots showing the optimal interaction sites of a hydrophobic probe (methyl of isopropanol) in an uncorrected grid (blue mesh; ΔG^{i}_{bind} = -1.5 kcal/mol) and after correction (red transparent surface; ΔG^{i}_{corr} = -0.7 kcal/mol). The ligand (yellow sticks; PDB code 2XDK) is displayed for reference purposes only. The protein is displayed in the grey cartoon (backbone) and lines (atoms), except for Asp93, shown in the sticks (*A higher resolution / colour version of this figure is available in the electronic copy of the article*).

the expected atomic contribution for real ligands [18]. Thus, we conclude that the correction works as expected, eliminating artefacts due to the interdependence of the various atoms in a solvent molecule used as a probe and removing the size-dependency of the uncorrected atomic contributions. In consequence, the corrected free energy grids are much better suited to guide the rational design of ligands to macromolecular targets, particularly when there is no previous information about ligands.

3.2. Example 2: Allosteric Site of GA1

Glutaric acidemia type I (also called glutaric aciduria type I, GA1) is a rare but serious inherited disorder in which the body is unable to process certain amino acids properly.

GA1 patients have inadequate levels of the mitochondrial enzyme glutaryl-CoA dehydrogenase (GCDH), which helps break down the amino acids lysine, hydroxylysine, and tryptophan. Excessive levels of these amino acids and their intermediate breakdown products in the blood, urine, and tissues can be toxic, causing severe health problems [22, 23]. The clinical course of GA1 often features an episode of acute metabolic encephalopathy, which results in irreversible striatal injury. A burdensome dietary and pharmacological treatment does not prevent devastating neurological complications in at least 15 % of the patients [22, 23]. GCDH deficiency often occurs due to mutation-induced protein misfolding [24]. Therefore, the rescue of the misfolded proteins by pharmacological chaperones is a promising novel therapeutic approach for GA1.

The structure of Human Glutaryl-CoA Dehydrogenase in complex with the cofactor FAD (PDB code 1SIQ) was used as a starting point for the simulation to generate the biological (homotetramer) from the single-chain found in the asymmetric unit. FAD was kept in the MD simulation because the interest was to find allosteric ligands that would not compete with the substrate or the cofactor. In this case, we used ethanol as probe solvent, using a pre-equilibrated box of ethanol/water at 20 % (v/v), as described [17]. As shown in Fig. (**3**), a preferred binding site for ethanol was found near Thr65, but originally it appeared too small to offer significant binding opportunities for a drug-like ligand. After subsequent correction of the free energy values with the above-described procedure, three additional hydrophobic hot spots emerged. They were largely caused by a conformational change of the side-chains of Lys313 and Asn248, which opened up a large hydrophobic patch. This illustrates another advantage of MDmix as a binding-site mapper: as the protein is allowed a significant amount of conformational flexibility [16], the presence of hydrophobic probe solvents facilitates the opening of cryptic pockets [25-29]. As the polar head of ethanol shows a scarce affinity for the emerged hydrophobic patch, in the absence of the correction, the apparent affinity of the methyl group was underestimated. The centre of four binding hot spots was used to define pharmacophoric points (1 hydrogen bond acceptor, plus three hydrophobic groups) that were used as restraints in a docking-based virtual screening with the rDock program [30].

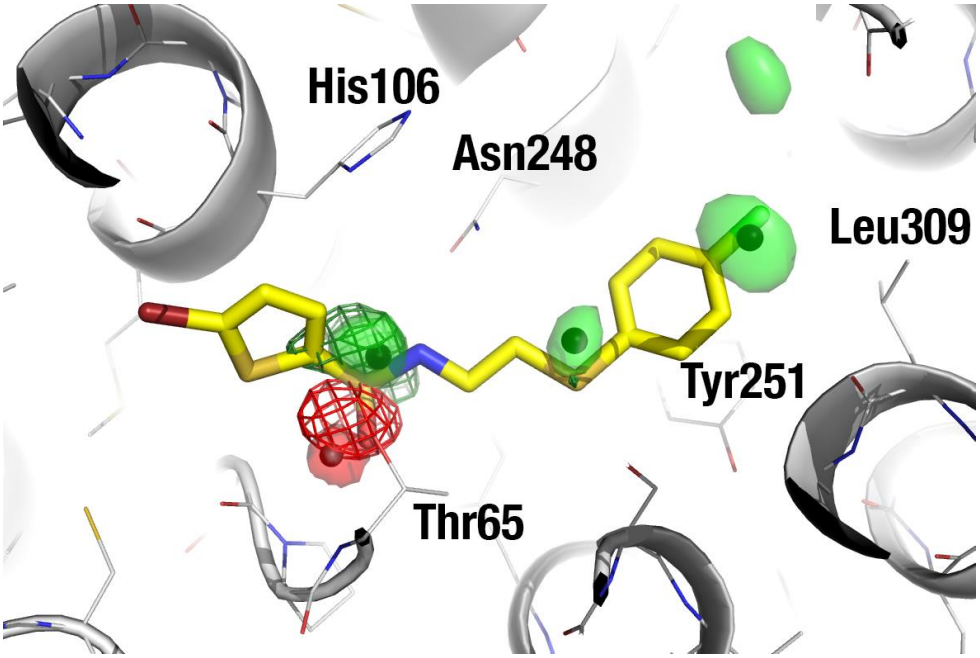

Fig. (3). Contour plots showing the optimal interaction sites of a hydrophobic probe (methyl of ethanol; green mesh) and a polar probe (hydroxyl of ethanol; red mesh), both at ΔG_{bind} = -1.5 kcal/mol. They identify a preferred binding site for ethanol next to Thr65. However, the site appears to lack any additional binding hot spot, suggesting that it is too small to be druggable. After correction, the hot spots are maintained (red and green transparent surfaces; ΔG_{corr} = -1.0 kcal/mol), but three additional hydrophobic hot spots emerge, revealing that the binding site offers substantial binding opportunities to a drug-like ligand. The centre of the corrected hot spots used to define a pharmacophore are shown as black dots. The ligand shown in yellow is an example virtual screening hit (*A higher resolution / colour version of this figure is available in the electronic copy of the article*).

CONCLUSION

Mixed solvent techniques have become quite popular [13, 31]. However, there is no consensus yet on the conditions that should be used, including the type of solvents, concentrations, use of solvent-solvent repulsive potentials, protein conformational restraints, length of simulations, etcetera. Furthermore, the technique is fundamentally used in a qualitative way. This may be sufficient to elucidate binding sites (the main use reported so far) but falls short for more quantitative application. Here we have presented a method to decompose the binding free energy (a molecular property) into atomic contributions that are more accurate and transferable to larger ligands. An alternative approach to ensure transferability is to simulate a very large set of solvent probes, each representing a chemical moiety present in typical drugs. This was recently demonstrated by Yanagisawa and co-workers using a set of 138 cosolvents [32]. Simulation of a much smaller set of cosolvents containing the essential atom types, followed by atomic partitioning of $\Delta G_{bind,}$ is far more efficient [33, 34]. When using non-corrected atomic contributions, cosolvent-based simulations can yield relative binding affinities as accurate as the free energy perturbation (FEP) methods, which are considered the gold standard in structure-based drug design [35]. The atomic repartition scheme presented here should bring about a further increase in accuracy [15]. Besides the theoretical background of the partitioning scheme, here, we have illustrated the improvement in the predictions with two visual examples. Future articles will disclose practical applications of the method and investigate the use of said atomic contributions to predict (relative) binding free energies on congeneric series of ligands.

ETHICS APPROVAL AND CONSENT TO PARTICIPATE

Not applicable.

HUMAN AND ANIMAL RIGHTS

No animals/humans were used for studies that are the basis of this research.

CONSENT FOR PUBLICATION

Not applicable.

AVAILABILITY OF DATA AND MATERIALS

The data supporting the findings of the article is available within the article.

FUNDING

None.

CONFLICT OF INTEREST

The authors declare no conflict of interest, financial or otherwise.

ACKNOWLEDGEMENTS

Declared none.

REFERENCES

[1] de Ruiter A, Oostenbrink C. Free energy calculations of protein-ligand interactions. Curr Opin Chem Biol 2011; 15(4): 547-52. http://dx.doi.org/10.1016/j.cbpa.2011.05.021 PMID: 21684797

[2] Kitchen DB, Decornez H, Furr JR, Bajorath J. Docking and scoring in virtual screening for drug discovery: Methods and applications. Nat Rev Drug Discov 2004; 3(11): 935-49. http://dx.doi.org/10.1038/nrd1549 PMID: 15520816

[3] De Vivo M, Masetti M, Bottegoni G, Cavalli A. Role of molecular dynamics and related methods in drug discovery. J Med Chem 2016; 59(9): 4035-61. http://dx.doi.org/10.1021/acs.jmedchem.5b01684 PMID: 26807648

[4] Pan AC, Xu H, Palpant T, Shaw DE. Quantitative characterization of the binding and unbinding of millimolar drug fragments with molecular dynamics simulations. J Chem Theory Comput 2017; 13(7): 3372-7. http://dx.doi.org/10.1021/acs.jctc.7b00172 PMID: 28582625

[5] Pan AC, Borhani DW, Dror RO, Shaw DE. Molecular determinants of drug-receptor binding kinetics. Drug Discov Today 2013; 18(13-14): 667-73. http://dx.doi.org/10.1016/j.drudis.2013.02.007 PMID: 23454741

[6] Kokh DB, Amaral M, Bomke J, *et al.* Estimation of drug-target residence times by τ-random acceleration molecular dynamics simulations. J Chem Theory Comput 2018; 14(7): 3859-69. http://dx.doi.org/10.1021/acs.jctc.8b00230 PMID: 29768913

[7] Casasnovas R, Limongelli V, Tiwary P, Carloni P, Parrinello M. Unbinding kinetics of a p38 MAP kinase type II inhibitor from metadynamics simulations. J Am Chem Soc 2017; 139(13): 4780-8. http://dx.doi.org/10.1021/jacs.6b12950 PMID: 28290199

[8] Plattner N, Doerr S, De Fabritiis G, Noé F. Complete protein-protein association kinetics in atomic detail revealed by molecular dynamics simulations and Markov modelling. Nat Chem 2017; 9(10): 1005-11. http://dx.doi.org/10.1038/nchem.2785 PMID: 28937668

[9] Seco J, Luque FJ, Barril X. Binding site detection and druggability index from first principles. J Med Chem 2009; 52(8): 2363-71. http://dx.doi.org/10.1021/jm801385d PMID: 19296650

[10] Guvench O, MacKerell AD Jr. Computational fragment-based binding site identification by ligand competitive saturation. PLOS Comput Biol 2009; 5(7): e1000435. http://dx.doi.org/10.1371/journal.pcbi.1000435 PMID: 19593374

[11] Byerly DW, McElroy CA, Foster MP. Mapping the surface of *Escherichia coli* peptide deformylase by NMR with organic solvents. Protein Sci 2002; 11(7): 1850-3. http://dx.doi.org/10.1110/ps.0203402 PMID: 12070337

[12] Mattos C, Bellamacina CR, Peisach E, *et al.* Multiple solvent crystal structures: Probing binding sites, plasticity and hydration. J Mol Biol 2006; 357(5): 1471-82. http://dx.doi.org/10.1016/j.jmb.2006.01.039 PMID: 16488429

[13] Ghanakota P, Carlson HA. Driving structure-based drug discovery through cosolvent molecular dynamics. J Med Chem 2016; 59(23): 10383-99. http://dx.doi.org/10.1021/acs.jmedchem.6b00399 PMID: 27486927

[14] Patel Y, Gillet VJ, Howe T, Pastor J, Oyarzabal J, Willett P. Assessment of additive/nonadditive effects in structure-activity relationships: Implications for iterative drug design. J Med Chem 2008; 51(23): 7552-62. http://dx.doi.org/10.1021/jm801070q PMID: 19012393

[15] Barril Alonso X, Alvarez Garcia D, Schmidtke P. Method of binding site and binding energy determination by mixed explicit solvent simulations WO2013092922A2, 2012.

[16] Alvarez-Garcia D, Barril X. Relationship between protein flexibility and binding: Lessons for structure-based drug design. J Chem Theory Comput 2014; 10(6): 2608-14. http://dx.doi.org/10.1021/ct500182z PMID: 26580781

[17] Alvarez-Garcia D, Barril X. Molecular simulations with solvent competition quantify water displaceability and provide accurate interaction maps of protein binding sites. J Med Chem 2014; 57(20): 8530-9. http://dx.doi.org/10.1021/jm5010418 PMID: 25275946

[18] Kuntz ID, Chen K, Sharp KA, Kollman PA. The maximal affinity of ligands. Proc Natl Acad Sci USA 1999; 96(18): 9997-10002. http://dx.doi.org/10.1073/pnas.96.18.9997 PMID: 10468550

[19] Janin YL. Heat shock protein 90 inhibitors. A text book example of medicinal chemistry? J Med Chem 2005; 48(24): 7503-12. http://dx.doi.org/10.1021/jm050759r PMID: 16302791

[20] Ruiz-Carmona S, Schmidtke P, Luque FJ, *et al.* Dynamic undocking and the quasi-bound state as tools for drug discovery. Nat Chem 2017; 9(3): 201-6. http://dx.doi.org/10.1038/nchem.2660 PMID: 28221352

[21] Murray CW, Carr MG, Callaghan O, *et al.* Fragment-based drug discovery applied to Hsp90. Discovery of two lead series with high ligand efficiency. J Med Chem 2010; 53(16): 5942-55. http://dx.doi.org/10.1021/jm100059d PMID: 20718493

[22] Boy N, Mühlhausen C, Maier EM, *et al.* Proposed recommendations for diagnosing and managing individuals with glutaric aciduria type I: Second revision. J Inherit Metab Dis 2017; 40(1): 75-101. http://dx.doi.org/10.1007/s10545-016-9999-9 PMID: 27853989

[23] Mosaeilhy A, Mohamed MM, C GPD, *et al.* Genotype-phenotype correlation in 18 Egyptian patients with glutaric acidemia type I. Metab Brain Dis 2017; 32(5): 1417-26. http://dx.doi.org/10.1007/s11011-017-0006-4 PMID: 28389991

[24] Schmiesing J, Lohmöller B, Schweizer M, *et al.* Disease-causing mutations affecting surface residues of mitochondrial glutaryl-CoA dehydrogenase impair stability, heteromeric complex formation and mitochondria architecture. Hum Mol Genet 2017; 26(3): 538-51. http://dx.doi.org/10.1093/hmg/ddw411 PMID: 28062662

[25] Oleinikovas V, Saladino G, Cossins BP, Gervasio FL. Understanding cryptic pocket formation in protein targets by enhanced sampling simulations. J Am Chem Soc 2016; 138(43): 14257-63. http://dx.doi.org/10.1021/jacs.6b05425 PMID: 27726386

[26] Kimura SR, Hu HP, Ruvinsky AM, Sherman W, Favia AD. Deciphering cryptic binding sites on proteins by mixed-solvent molecular dynamics. J Chem Inf Model 2017; 57(6): 1388-401. http://dx.doi.org/10.1021/acs.jcim.6b00623 PMID: 28537745

[27] Ghanakota P, van Vlijmen H, Sherman W, Beuming T. Large-scale validation of mixed-solvent simulations to assess hotspots at protein-protein interaction interfaces. J Chem Inf Model 2018; 58(4): 784-93. http://dx.doi.org/10.1021/acs.jcim.7b00487 PMID: 29617116

[28] Schmidt D, Boehm M, McClendon CL, Torella R, Gohlke H. Cosolvent-enhanced sampling and unbiased identification of cryptic pockets suitable for structure-based drug design. J Chem Theory Comput 2019; 15(5): 3331-43. http://dx.doi.org/10.1021/acs.jctc.8b01295 PMID: 30998331

[29] Smith RD, Carlson HA. Identification of cryptic binding sites using mixmd with standard and accelerated molecular dynamics. J Chem Inf Model 2021; 61(3): 1287-99. http://dx.doi.org/10.1021/acs.jcim.0c01002 PMID: 33599485

[30] Ruiz-Carmona S, Alvarez-Garcia D, Foloppe N, *et al.* rDock: A fast, versatile and open source program for docking ligands to proteins and nucleic acids. PLOS Comput Biol 2014; 10(4): e1003571. http://dx.doi.org/10.1371/journal.pcbi.1003571 PMID: 24722481

[31] Defelipe LA, Arcon JP, Modenutti CP, Marti MA, Turjanski AG, Barril X. Solvents to fragments to drugs: MD applications in drug design. Molecules 2018; 23(12): 1-14. http://dx.doi.org/10.3390/molecules23123269 PMID: 30544890

[32] Yanagisawa K, Moriwaki Y, Terada T, Shimizu K. Exprorer: Rational cosolvent set construction method for cosolvent molecular dynamics using large-scale computation. J Chem Inf Model 2021; 61(6): 2744-53. http://dx.doi.org/10.1021/acs.jcim.1c00134 PMID: 34061535

[33] Arcon JP, Defelipe LA, Modenutti CP, *et al.* Molecular dynamics in mixed solvents reveals protein-ligand interactions, Improves docking, and allows accurate binding free energy predictions. J Chem Inf Model 2017; 57(4): 846-63.

http://dx.doi.org/10.1021/acs.jcim.6b00678 PMID: 28318252

[34] Arcon JP, Defelipe LA, Lopez ED, *et al.* Cosolvent-based protein pharmacophore for ligand enrichment in virtual screening. J Chem Inf Model 2019; 59(8): 3572-83.
http://dx.doi.org/10.1021/acs.jcim.9b00371 PMID: 31373819

[35] Goel H, Hazel A, Ustach VD, Jo S, Yu W, MacKerell AD Jr. Rapid and accurate estimation of protein-ligand relative binding affinities using site-identification by ligand competitive saturation. Chem Sci (Camb) 2021; 12(25): 8844-58.
http://dx.doi.org/10.1039/D1SC01781K PMID: 34257885